Proc. 18th Winter Workshop on
Nuclear Dynamics (2002) 000–000

18th Winter Workshop
on Nuclear Dynamics
Nassau, Bahamas
January 20–27, 2002

Systematics of Heavy Quark Production at RHIC

R. Vogt

Physics Department, University of California, Davis, CA 95616
and
Nuclear Science Division, Lawrence Berkeley National Laboratory
University of California, Berkeley, California 94720, USA

Abstract. We discuss a program for systematic studies of heavy quark production in pp, pA and AA interactions. The $Q\overline{Q}$ production cross sections themselves cannot be accurately predicted to better than 50% at RHIC. For studies of deviations in $Q\overline{Q}$ production such as those by nuclear shadowing and heavy quark energy loss, the pp cross section thus needs to be measured. We then show that the ratio of pA to pp dilepton mass distributions can provide a measurement of the nuclear gluon distribution. With total rates and nuclear shadowing under control it is easier to study energy loss and to use $c\overline{c}$ as a normalization of J/ψ production.

Keywords: relativistic heavy-ion collisions, heavy flavors
PACS: 25.75.-q

1. Introduction

It is important to have an accurate measure of the charm and bottom cross sections for several reasons. Heavy quark decays are expected to dominate the lepton pair continuum from the $J/\psi(c\overline{c})$ and $\Upsilon(b\overline{b})$ up to the mass of the Z^0 [1, 2, 3]. Thus the Drell-Yan yield and any thermal dilepton production will essentially be hidden by the heavy quark decay contributions [1]. The shape of the charm and bottom contributions to this continuum could be significantly altered by heavy quark energy loss [2, 4]. If the loss is large, it may be possible to extract a thermal dilepton yield if it cannot be determined by other means [5]. Heavy quark production in a quark-gluon plasma has also been predicted [6]. This additional yield can only be determined if the AA rate can be accurately measured. Finally, the total charm rate would be a useful reference for J/ψ production since enhancement of the J/ψ to total charm ratio has been predicted in a number of models [7, 8, 9, 10, 11, 12].

ISBN 963 00 0000 0

2. Baseline Rates in pp

We first discuss some new calculations of the $Q\overline{Q}$ total cross sections in pp collisions with the most recent nucleon parton distribution functions. At leading order (LO) heavy quarks are produced by gg fusion and $q\overline{q}$ annihilation while at next-to-leading order (NLO) qg and $\overline{q}g$ scattering is also included. To any order, the partonic cross section may be expressed in terms of dimensionless scaling functions $f_{ij}^{(k,l)}$ that depend only on the variable η [13],

$$\hat{\sigma}_{ij}(\hat{s},m_Q^2,\mu^2) = \frac{\alpha_s^2(\mu)}{m^2}\sum_{k=0}^{\infty}\left(4\pi\alpha_s(\mu)\right)^k\sum_{l=0}^{k} f_{ij}^{(k,l)}(\eta)\,\ln^l\left(\frac{\mu^2}{m_Q^2}\right), \tag{1}$$

where $\hat{s}$ is the partonic center of mass energy squared, m_Q is the heavy quark mass, μ is the scale and $\eta = \hat{s}/4m_Q^2 - 1$. The cross section is calculated as an expansion in powers of α_s with $k = 0$ corresponding to the Born cross section at order $O(\alpha_s^2)$. The first correction, $k = 1$, corresponds to the NLO cross section at $O(\alpha_s^3)$. It is only at this order and above that the dependence on renormalization scale, μ_R, enters the calculation since when $k = 1$ and $l = 1$, the logarithm $\ln(\mu^2/m_Q^2)$ appears. The dependence on the factorization scale, μ_F, the argument of α_s, appears already at LO. We assume that $\mu_R = \mu_F = \mu$. The next-to-next-to-leading order (NNLO) corrections to next-to-next-to-leading logarithm have been calculated near threshold [13] but the complete calculation only exists to NLO.

The total hadronic cross section is obtained by convoluting the total partonic cross section with the parton distribution functions (PDFs) of the initial hadrons,

$$\sigma_{pp}(s,m_Q^2) = \sum_{i,j=q,\overline{q},g}\int_{\frac{4m_Q^2}{s}}^{1}\frac{d\tau}{\tau}\,\delta(x_1x_2-\tau)\,F_i^p(x_1,\mu^2)F_j^p(x_2,\mu^2)\,\hat{\sigma}_{ij}(\tau,m_Q^2,\mu^2), \tag{2}$$

where the sum i is over all massless partons and x_1 and x_2 are fractional momenta. The PDFs, denoted by F_i^p, are evaluated at scale μ. All our calculations are fully NLO, applying NLO parton distribution functions and the two-loop α_s to both the $O(\alpha_s^2)$ and $O(\alpha_s^3)$ contributions, as is typically done [13, 14].

To obtain the pp cross sections at RHIC and LHC, we first compare the NLO cross sections to the available $c\overline{c}$ and $b\overline{b}$ production data by varying the mass, m_Q, and scale, μ, to obtain the 'best' agreement with the data for several combinations of m_Q, μ, and PDF. We use the recent MRST HO central gluon [16], CTEQ 5M [17], and GRV 98 HO [18] distributions. The results for the $c\overline{c}$ cross section in pp interactions is shown in Fig. 1. On the left-hand side, $\mu = m_c$ for $1.2 \le m_c \le 1.8$ GeV, while on the right-hand side, $\mu = 2m_c$ for the same masses, all calculated with MRST HO. The scale is not decreased below m_c because the minimum scale in the PDF is larger than $m_c/2$. The cross sections with $\mu = m_c$ are all larger than those with $\mu = 2m_c$ for the same m_c because $\alpha_s(m_c) > \alpha_s(2m_c)$ by virtue of the running of α_s. Evolution of the PDFs with μ tends to go in the opposite direction. At higher scales the two effects tend to compensate and reduce the scale dependence but the charm quark mass is not large enough for this to occur.

The best agreement with $\mu = m_c$ is for $m_c = 1.4$ GeV and $m_c = 1.2$ GeV is the best choice for $\mu = 2m_c$ for the MRST HO and CTEQ 5M distributions. The best agreement

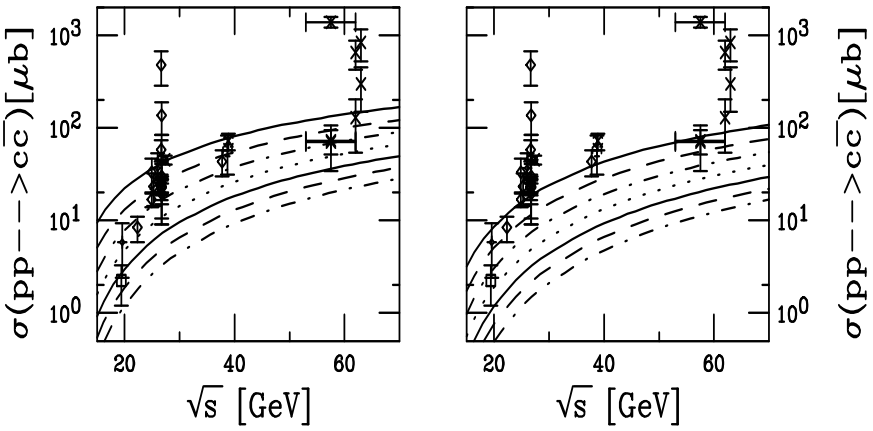

Fig. 1. Total $c\overline{c}$ cross sections in pp interactions up to ISR energies as a function of the charm quark mass. See [15] for references to the data. All calculations are fully NLO using the MRST HO (central gluon) parton densities. The left-hand plot shows the results with $\mu = m_c$ while in the right-hand plot $\mu = 2m_c$. From top to bottom the curves are $m_c = 1.2$, 1.3, 1.4, 1.5, 1.6, 1.7, and 1.8 GeV.

with GRV 98 HO is $\mu = m_c = 1.3$ GeV while the results with $\mu = 2m_c$ lie below the data for all m_c. All five results agree very well with each other for $pp \to c\overline{c}$, as shown on the left side of Fig. 2. There is more of a spread in the $\pi^- p \to c\overline{c}$ results, shown on the right side of Fig. 2. This is because the π^- PDFs are not very well known. The last evaluations, SMRS [19], Owens-π [20], and GRV-π [21] were 10-15 years ago and do not reflect any of the latest information on the low x behavior of the proton PDFs, *e.g.* the distributions are all flat as $x \to 0$ with no low x rise. These pion evaluations also depend on the behavior of the proton PDFs used in the original fit, including the value of $\Lambda_{\rm QCD}$. Thus the pion and proton PDFs are generally incompatible. Note that the $\pi^- p$ cross sections are a bit lower than the data compared to the pp cross sections, suggesting that lighter quark masses would tend to be favored for this data. The reason is because the low x rise in the proton PDFs depletes the gluon density for $x > 0.02$ relative to a constant at $x \to 0$ for $\mu = \mu_0$ the initial scale of the PDF. The $\pi^- p$ data are in a relatively large x region, $0.1 \leq x = 2\mu/\sqrt{s} \leq 0.3$, where this difference is important.

We have tried to play the same game with the $b\overline{b}$ total cross sections but these have mostly been measured in $\pi^- p$ interactions. The typical x values of $b\overline{b}$ production are even larger than those for $c\overline{c}$ but it is not clear that $\pi^- p \to b\overline{b}$ also favors lower masses. At the fixed target energies of $b\overline{b}$ production, $q\overline{q}$ annihilation dominates while gg fusion is still most important for $c\overline{c}$ production [22]. The valence-valence $\overline{u}_\pi u_p$ contribution is most important since valence distributions dominate at large x. For all three PDFs used, we find $m_b = \mu = 4.75$ GeV, $m_b = \mu/2 = 4.5$ GeV, and $m_b = 2\mu = 5$ GeV most compatible with the sparse data. Attempts to measure the $b\overline{b}$ total cross section in fixed-target pp interactions have been less successful. Hopefully the HERA-B experiment at DESY [23] will soon

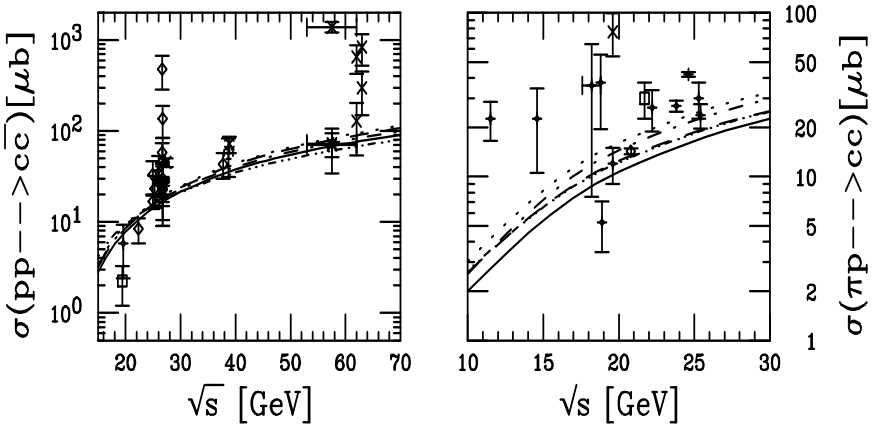

Fig. 2. Total $c\overline{c}$ cross sections in pp (left) and $\pi^- p$ interactions compared to data. See [15] for references (right) to the data. All calculations are fully NLO. The curves are: MRST HO (central gluon) with $\mu = m = 1.4$ GeV (solid) and $\mu = 2m = 2.4$ GeV (dashed); CTEQ 5M with $\mu = m = 1.4$ GeV (dot-dashed) and $\mu = 2m = 2.4$ GeV (dotted); and GRV 98 HO with $\mu = m = 1.3$ GeV (dot-dot-dot-dashed).

provide a new measurement.

Our calculations can then be extrapolated to RHIC and LHC energies. The result for $c\overline{c}$ is shown in Fig. 3. Even though the cross sections agree within 30% at 40 GeV, by the Pb+Pb energy of the LHC they differ by a factor of 2.3. The spread in the $b\overline{b}$ cross sections is considerably smaller, $\sim 20-30\%$ at the ion collider energies. Our results for pp interactions at 40 GeV, 200 GeV, and 5.5 TeV are given in Table 1. The AA rates per event at $b = 0$ with the same energies can be obtained by multiplying these cross sections by $T_{AA}(b = 0)$, 29.3/mb for Au+Au and 30.4/mb for Pb+Pb. We find 8-13 $c\overline{c}$ pairs and ~ 0.05 $b\overline{b}$ pairs at RHIC with 97-225 $c\overline{c}$ pairs and ~ 5 $b\overline{b}$ pairs at LHC without nuclear shadowing. The shadowing effect is rather small for $c\overline{c}$ at RHIC and actually enhances the $b\overline{b}$ rate. The only important modification due to shadowing in the total cross section is on the $c\overline{c}$ rate at the LHC which is reduced to 67-150 pairs. Energy loss does not affect the total rate [4]. As noted by Thews, this $c\overline{c}$ rate is large enough at RHIC for independent c and $\overline{c}$ quarks to dynamically recombine to form J/ψ's [11]. The baseline rates of $Q\overline{Q}$ production are thus important for studying these effects.

3. Nuclear Gluon Distribution in pA

We now turn to a calculation of the nuclear gluon distribution in pA interactions [27]. We show that the dilepton continuum can be used to study nuclear shadowing and reproduces the input shadowing function well, in this case, the EKS98 parameterization [28]. To simplify notation, we refer to generic heavy quarks, Q, and heavy-flavored mesons, H. The

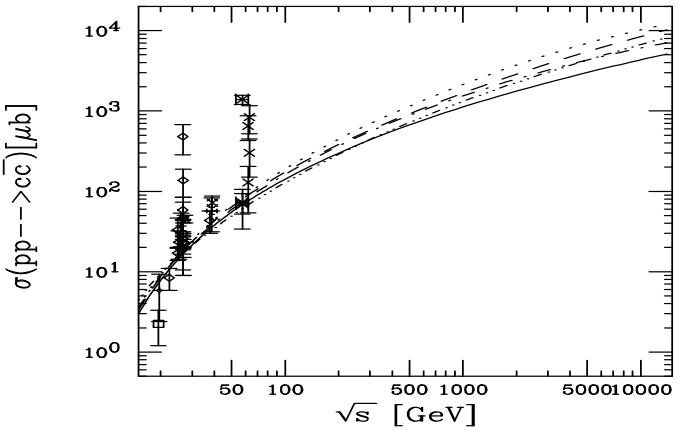

Fig. 3. Total $c\overline{c}$ cross sections in pp interactions up to 14 TeV. See [15] for references to the data. All calculations are fully NLO. The curves are the same as in Fig. 2.

lepton pair production cross section is

$$\begin{aligned}\frac{d\sigma^{pA\to l\bar{l}+X}}{dM_{l\bar{l}}dy_{l\bar{l}}} &= \int d^3\vec{p}_l d^3\vec{p}_{\overline{l}} \int d^3\vec{p}_H d^3\vec{p}_{\overline{H}}\,\delta(M_{l\bar{l}}-M(p_l,p_{\overline{l}}))\,\delta(y_{l\bar{l}}-y(p_l,p_{\overline{l}})) \\ &\quad\times\frac{d\Gamma^{H\to l+X}(\vec{p}_H)}{d^3\vec{p}_l}\,\frac{d\Gamma^{\overline{H}\to\overline{l}+X}(\vec{p}_{\overline{H}})}{d^3\vec{p}_{\overline{l}}}\,\frac{d\sigma^{pA\to H\overline{H}+X}}{d^3\vec{p}_H d^3\vec{p}_{\overline{H}}} \\ &\quad\times\theta(y_{\min}<y_l,y_{\overline{l}}<y_{\max})\theta(\phi_{\min}<\phi_l,\phi_{\overline{l}}<\phi_{\max}) \qquad (3)\end{aligned}$$

where $M(p_l,p_{\overline{l}})$ and $y(p_l,p_{\overline{l}})$ are the invariant mass and rapidity of the $l\bar{l}$ pair. The decay rate, $d\Gamma^{H\to l+X}(\vec{p}_H)/d^3\vec{p}_l$, is the probability that meson H with momentum $\vec{p}_H$ decays to a lepton l with momentum $\vec{p}_l$. The θ functions define single lepton rapidity and azimuthal angle cuts used to simulate detector acceptances.

Using a fragmentation function D_Q^H to describe quark fragmentation to mesons, the $H\overline{H}$ production cross section can be written as

$$\begin{aligned}\frac{d\sigma^{pA\to H\overline{H}+X}}{d^3\vec{p}_H d^3\vec{p}_{\overline{H}}} &= \int\frac{d^3\vec{p}_Q}{E_Q}\frac{d^3\vec{p}_{\overline{Q}}}{E_{\overline{Q}}}E_Q E_{\overline{Q}}\frac{d\sigma^{pA\to Q\overline{Q}+X}}{d^3\vec{p}_Q d^3\vec{p}_{\overline{Q}}}\int dz_1 dz_2 D_Q^H(z_1)D_{\overline{Q}}^{\overline{H}}(z_2) \\ &\times\quad\delta^{(3)}(\vec{p}_H-z_1\vec{p}_Q)\,\delta^{(3)}(\vec{p}_{\overline{H}}-z_2\vec{p}_{\overline{Q}})\,. \qquad (4)\end{aligned}$$

Our calculations were done with two different fragmentation functions. We found that our results were independent of D_Q^H. The hadronic heavy quark production cross section *per nucleon* in pA collisions can be factorized into the general form

$$\frac{1}{A}E_Q E_{\overline{Q}}\frac{d\sigma^{pA\to Q\overline{Q}+X}}{d^3\vec{p}_Q d^3\vec{p}_{\overline{Q}}} = \sum_{i,j}\int dx_1 dx_2\, f_i^p(x_1,\mu^2)\,f_j^A(x_2,\mu^2)E_Q E_{\overline{Q}}\frac{d\hat{\sigma}^{ij\to Q\overline{Q}}}{d^3\vec{p}_Q d^3\vec{p}_{\overline{Q}}} \qquad (5)$$

Table 1. Charm and bottom total cross sections per nucleon for the extrapolated calculations shown previously. The heavy quark mass and factorization/renormalization scales are given, along with the cross sections at 40 GeV (HERA-B), 200 GeV (Au+Au at RHIC), and 5.5 TeV (Pb+Pb at LHC).

			40 GeV	200 GeV	5.5 TeV
		$c\overline{c}$			
PDF	m_c (GeV)	μ/m_c	σ (μb)	σ (μb)	σ (mb)
MRST HO	1.4	1	37.8	298	3.18
MRST HO	1.2	2	43.0	382	5.83
CTEQ 5M	1.4	1	40.3	366	4.52
CTEQ 5M	1.2	2	44.5	445	7.39
GRV 98 HO	1.3	1	34.9	289	4.59
		$b\overline{b}$			
PDF	m_b (GeV)	μ/m_b	σ (nb)	σ (μb)	σ (μb)
MRST HO	4.75	1	9.82	1.90	185.2
MRST HO	4.5	2	8.73	1.72	193.2
MRST HO	5.0	0.5	10.96	2.16	184.8
GRV 98 HO	4.75	1	13.40	1.65	177.6
GRV 98 HO	4.5	2	12.10	1.64	199.0
GRV 98 HO	5.0	0.5	14.80	1.73	166.0

where $f_i^p = F_i^p/x$ and $f_i^A = F_i^A/x$ with $F_i^A = F_i^p R_i^A$. The shadowing ratio R_i^A is that of EKS98 [28]. The partonic cross section is the differential of Eq. (1) at $k = 0$. Note that the total lepton pair production cross section is equal to the total $Q\overline{Q}$ cross section multiplied by the square of the lepton branching ratio.

We compare the ratios of lepton pair cross sections with the input R_g^A in Fig. 4. All the results are integrated over the rapidity intervals appropriate to the PHENIX and ALICE dilepton coverages. The ratio follows R_g^A at all energies. The higher the energy, the better the agreement: at the LHC the two agree very well.

The ratio always lies below R_g^A for two reasons. First, $q\overline{q}$ annihilation is included and quark shadowing is different than gluon shadowing. The $q\overline{q}$ contribution decreases with energy, leading to better agreement at the LHC. Second, the phase space integration smears the shadowing effect relative to $R_g^A(\langle x_2\rangle, \langle\mu\rangle)$. Note that the ratio deviates slightly more from $R_g^A(\langle x_2\rangle, \langle\mu\rangle)$ for e^+e^- than for $\mu^+\mu^-$ because the curvature of R_g^A with x is stronger at larger values of x and, due to the differences in rapidity coverage, the average values of x_2 are larger for e^+e^-.

The average x_2 decreases with energy. We have $0.14 \leq \langle x_2\rangle \leq 0.32$ at the SPS where R_g^A is decreasing. At RHIC, $0.003 \leq \langle x_2\rangle \leq 0.012$, where R_g^A is increasing quite rapidly. Finally, at the LHC, $3\times10^{-5} \leq \langle x_2\rangle \leq 2\times10^{-4}$ where R_g^A is almost independent of x. The values of $\langle x_2\rangle$ are typically larger for electron pairs at collider energies because the electron

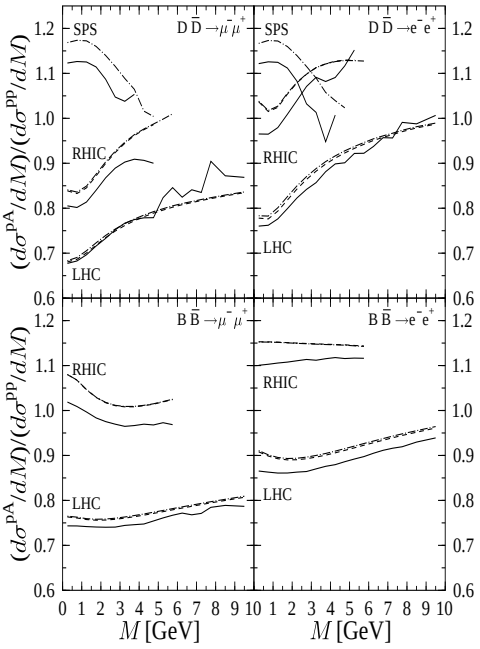

Fig. 4. The ratios of lepton pairs from correlated $D\overline{D}$ and $B\overline{B}$ decays in pA to pp collisions at the same energies (solid curves) compared to the input R_g^A at the average x_2 and μ (dashed)/$\sqrt{\langle\mu^2\rangle}$ (dot-dashed) of each M bin. From Ref. [27].

coverage is more central than the muon coverage.

The average μ^2 increases with energy and quark mass. For $c\overline{c}$ we have $7.58 \leq \langle\mu^2\rangle \leq 48.5$ GeV^2 at the SPS, $9.46 \leq \langle\mu^2\rangle \leq 141$ GeV^2 at RHIC, and $11.4 \leq \langle\mu^2\rangle \leq 577$ GeV^2 at the LHC. For $b\overline{b}$ production, $32.0 \leq \langle\mu^2\rangle \leq 54.3$ GeV^2 at RHIC and $37.9 \leq \langle\mu^2\rangle \leq 156$ GeV^2 at LHC.

4. Heavy Quarks in *AA*

4.1. Effects of Energy Loss

Energy loss would best be determined by reconstruction of D and B meson decays and comparing with distributions expected from pp and pA extrapolations that do not consider energy loss. Whether energy loss is measurable in reconstructed D and B decays or not, the change in the dilepton continuum should surely be present if the loss is nonzero and will bias the interpretation of the dilepton continuum. So far, the amount of the energy lost by heavy quarks is unknown. While a number of calculations have been made of the collisional

loss in a quark-gluon plasma [29], only recently has radiative loss been applied to heavy quarks [30]. The radiative loss can be rather large, $dE/dx \sim -5$ GeV/fm for a 10 GeV heavy quark, and increasing with energy, but the collisional loss is smaller, $dE/dx \sim 1-2$ GeV/fm, and nearly independent of energy [30]. We note that energy loss will suppress high p_T and large invariant mass quark pairs as long as $|dE/dx| \geq \langle p_T \rangle / R_A$ [4].

It is important to note that energy loss does not reduce the number of $Q\overline{Q}$ pairs produced but only changes their momentum. However, an effective reduction in the observed heavy quark yield can be expected in a finite acceptance detector because fewer leptons from the subsequent decays of the heavy quarks will pass kinematic cuts such as a minimum lepton p_T.

If the loss or the p_T cut is large, the Drell-Yan and thermal dileptons could emerge from under the reduced $D\overline{D}$ and $B\overline{B}$ decay contributions at large masses. Even without considering energy loss, Gallmeister *et al.* suggested that thermal dileptons could be detected by increasing the minimum lepton p_T because, in the D and B rest frames, the maximum energy of the individual leptons is limited to 0.9 and 2.2 GeV respectively. The lepton p_T from thermal production has no such limitation [5].

4.2. Quarkonium normalization

Heavy quark production in AA collisions is also interesting because of the prominent effect it could have on quarkonium. Initial nucleon-nucleon collisions may not be the only source of quarkonium production. Regeneration of quarkonium in the plasma phase [7, 8, 9, 10, 11, 12] could counter the effects of suppression, ultimately leading to enhanced quarkonium production. In the plasma phase, there are two basic approaches: statistical and dynamical coalescence. Both these approaches depend on being able to measure the quarkonium rate relative to total $Q\overline{Q}$ production. Thus the $Q\overline{Q}$ rate is preferable as a normalization of quarkonium production, particularly since both share the same production mechanisms and approximate $\langle x \rangle$, $\langle \mu \rangle$ values. However the final-state effects such as energy loss will make the total rate difficult to quantify without substantial detailed studies. These secondary production models should be testable already at RHIC where enhancements of factors of 2-3 are expected from coalescence [9, 11].

Other processes besides heavy quark production have been suggested as references for quarkonium production. Using the Z^0 as a reference [31] as a reference would eliminate the uncertainty due to final-state effects on the $Z^0 \to l^+ l^-$ decays but the different production mechanisms and masses leaves it less desirable. It has also been suggested that the $\psi'/J/\psi$ and Υ'/Υ ratios be studied as a function of p_T [32] since deviations from the pp ratios should reflect quark-gluon plasma characteristics. The only drawback to such a mechanism is that strong suppression may result in poor statistics.

Acknowledgements

I would like to thank K.J. Eskola and V.J. Kolhinen for collaboration on part of this work. This work was supported by the Director, Office of Energy Research, Office of High Energy

and Nuclear Physics, Nuclear Physics Division of the U.S. Department of Energy under Contract No. DE-AC03-76SF00098.

References

1. S. Gavin, P.L. McGaughey, P.V. Ruuskanen and R. Vogt, *Phys. Rev.* **C54** 2606, (1996).
2. I.P. Lokhtin and A.M. Snigirev, *Eur. Phys. J.* **C21** (2001) 155.
3. G. Baur *et al.*, CMS NOTE 2000/060.
4. Z. Lin and R. Vogt, *Nucl. Phys.* **B544** (1999) 339.
5. K. Gallmeister, B. Kämpfer and O.P. Pavlenko, *Eur. Phys. J.* **C8** (1999) 473.
6. A. Shor, *Phys. Lett.* **B215** (1988) 375; *Phys. Lett.* **B233** (1989) 231; B. Müller and X.-N. Wang, *Phys. Rev. Lett.* **68** (1992) 2437; P. Lévai and R. Vogt, *Phys. Rev.* **C56** (1997) 2707.
7. P. Braun-Munzinger and J. Stachel, *Phys. Lett.* **B490** (2000) 196; *Nucl. Phys.* **A690** (2001) 119.
8. M.I. Gorenstein, A.P. Kostyuk, H. Stöcker and W. Greiner, *Phys. Lett.* **B509** (2001) 277; *J. Phys.* **G27** (2001) L47.
9. M.I. Gorenstein, A.P. Kostyuk, H. Stöcker and W. Greiner, hep-ph/0012292.
10. L. Grandchamp and R. Rapp, *Phys. Lett.* **B523** (2001) 60.
11. R.L. Thews, M. Schroedter and J. Rafelski, *Phys. Rev.* **C63** (2001) 054905.
12. R.L. Thews, in proceedings of 'Statistical QCD', Bielefeld, Aug. 2001, edited by F. Karsch *et al.*, hep-ph/0111015.
13. N. Kidonakis, E. Laenen, S. Moch and R. Vogt, *Phys. Rev.* **D64** (2001) 114001.
14. M.L. Mangano, P. Nason and G. Ridolfi, *Nucl. Phys.* **B405** (1993) 507.
15. P.L. McGaughey *et al.*, *Int. J. Mod. Phys.* **A10** (1995) 2999.
16. A.D. Martin, R.G. Roberts, W.J. Stirling and R.S. Thorne, *Eur. Phys. J.* **C4** (1998) 463; *Phys. Lett.* **B443** (1998) 301.
17. H.L. Lai *et al.*, *Eur. Phys. J.* **C12** (2000) 375.
18. M. Glück, E. Reya and A. Vogt, *Eur. Phys. J.* **C5** (1998) 461.
19. P.J. Sutton, A.D. Martin, R.G. Roberts and W.J. Stirling, *Phys. Rev.* **D45** (1992) 2349.
20. J.F. Owens, *Phys. Rev.* **D30** (1984) 943.
21. M. Glück, E. Reya and A. Vogt, *Z. Phys.* **C53** (1992) 651.
22. J. Smith and R. Vogt, *Z. Phys.* **C75** (1997) 271.
23. HERA-B Report on Status and Prospects, DESY-PRC 00/04.
24. R. Vogt, to appear in the Proceedings of the Hard Probe Collaboration, LBNL-45350, hep-ph/0111271.
25. S. Frixione, M.L. Mangano, P. Nason and G. Ridolfi, *Nucl. Phys.* **B431** (1994) 453.
26. M.L. Mangano, in proceedings of the 2001 CERN Workshop on Hard Probes in Heavy Ion Collisions at the LHC, Oct. 2001.
27. K.J. Eskola, V. Kolhinen and R. Vogt, *Nucl. Phys.* **A696** (2001) 729.
28. K.J. Eskola, V.J. Kolhinen and P.V. Ruuskanen, *Nucl. Phys.* **B535** 351, (1998); K.J.

Eskola, V.J. Kolhinen and C.A. Salgado, *Eur. Phys. J.* **C9** (1999) 61.
29. J.D. Bjorken, Fermilab Report No. PUB-82/59-THY (unpublished); B. Svetitsky, *Phys. Rev.* **D37** (1988) 2484; B. Svetitsky and A. Uziel, *Phys. Rev.* **D55** (1997) 2616; M.H. Thoma and M. Gyulassy, *Nucl. Phys.* **B351** (1991) 491; S. Mrówczyński, *Phys. Lett.* **B269** (1991) 383; Y. Koike and T. Matsui, *Phys. Rev.* **D45** (1992) 3237; M.H. Thoma, *Phys. Lett.* **B273** (1991) 128; E. Braaten and M.H. Thoma, *Phys. Rev.* **D44** (1991) R2625.
30. M.G. Mustafa, D. Pal, D.K. Srivastava and M.H. Thoma, *Phys. Lett.* **B428** (1998) 234.
31. R. Vogt, *Phys. Rev.* **C64** (2001) 044901.
32. J.F. Gunion and R. Vogt, *Nucl. Phys.* **B492** (1997) 301.